RSC Advances

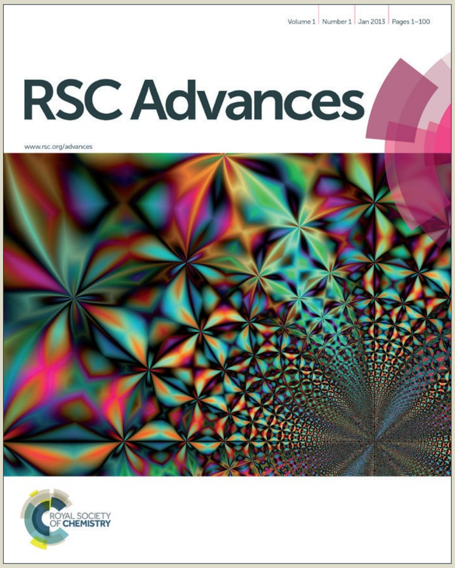

Volume 1 | Number 1 | Jan 2013 | Pages 1–100

RSC Advances

www.rsc.org/advances

ROYAL SOCIETY OF CHEMISTRY

RSC Advances

COMMUNICATION

A Polyimide-MWCNTs composite as high performance anode for aqueous Na-ion batteries

Received 00th January 20xx,
Accepted 00th January 20xx

DOI: 10.1039/x0xx00000x

www.rsc.org/

Tiantian Gu †, Min Zhou†, Mengyun Liu, Kangli Wang*, Shijie Cheng, Kai Jiang*

† These authors contributed equally to this work

A Polyimide-MWCNTs composite (PNP@CNTs) synthesized from 1, 4, 5, 8-naphthalenetetracarboxylic-dianhydride (NTCDA) and phenylene diamine (PDA) was investigated as a novel anode for aqueous Na-ion batteries. This composite demonstrates a high reversible capacity of 149 mAh g^{-1} at quite a low potential of - 0.65 V (vs SCE), superior rate capability and long-term cycling stability. The feasibility of PNP@CNTs in aqueous Na-ion full batteries is also confirmed in conjunction with the $Na_{0.44}$ MnO_2 cathode, possibly serving as a high performance aqueous Na host anode for large-scale electric energy storage applications.

1. Introduction

New types of energy storage technology are needed in conjunction with the development of renewable energy for efficient distribution of the electricity generated from renewable resources, such as sunlight or wind.[1, 2] For their integration with the electric grid, the rechargeable batteries should possess the advantages of low cost, safety, environmental friendliness, as well as long cycle life and high rate performances. In contrast, the energy density may address less concerns than the aforementioned aspects. Among various energy storage devices, Na-ion batteries (NIBs) have gained aroused interest for large-scale energy storage due to the abundant natural resources and low environmental impact.[3, 4] Moreover, constructing NIBs in aqueous electrolytes may be more favorable than those in conventional organic electrolytes for the intrinsic safety, low cost and high ionic conductivity of the aqueous electrolyte.[5-7] However, the limited electrochemical window of water raise the difficulties of developing appropriate anode and cathode materials. A number of host materials such as Mn-based oxides[8, 9] and Prussian blue type $Na_xM_yFe(CN)_6$ (M = Ni, Cu, etc.)[10-12] have been studied as cathodic hosts for aqueous Na-ion batteries and exhibit considerable electrochemical performances. However, the choose of anode materials is mainly limited to the NASICON-type $NaTi_2(PO_4)_3$.[13-15] Furthermore, these materials are all based on transitional metals which may bring serious cost and negative environmental impact for widespread applications.

Intensive efforts have been aimed at developing novel aqueous Na-host anode shifting from inorganic to organic compounds.[16, 17] Polyimide, a redox-active organic polymer with high mechanical strength, is considered to be a promising candidate for aqueous Na-ion batteries because of its resource abundance, structural diversity and stability in aqueous electrolyte. [18, 19] Furthermore, the flexible polymer backbone could provide higher mobility of the large-sized Na^+ which can effectively improve the poor kinetics of the Na^+ insertion/desertion reactions. [20-23]During the past years, various kinds of polyimide have been investigated as Na-host electrode, [24-26] but only few of them can work well in aqueous electrolytes due to the sloping high potential (above -0. 5 V vs SCE), [19, 27] thus resulting in low energy density in the practical full cells. As the electrochemical window of the aqueous electrolyte is quite narrow, it is of great importance to develop high performance polyimide anode with sufficiently low and flat redox potential. The electrochemical performance of redox-active polymer is strongly dependent on the polymer structure, thus designing highly conjugated polyimide skeleton by adjusting the dianhydride and diamine component can effectively optimize the redox potential of the polyimide.[18, 26] Based on this consideration, we focus on poly-(naphthalene four formyl phenylene diamine) (PNP), synthesized from 1,4,5,8-naphthalenetetracarboxylic dianhydride (NTCDA) and phenylene diamine (PDA). The unique structure of benzene ring (PDA) and naphthalene ring (NTCDA) will enlarge the π-conjugation system of the polymer backbone, thus resulting in a highly conjugated structure, which lead to a planar voltage plateau and high conductivity of the polymer backbone. Moreover, the electrochemical performance of PNP can be further improved by the addition of MWCNTs. The high conductivity and strong mechanical properties of the CNTs can not only provide a cross-

---

State Key Laboratory of Advanced Electromagnetic Engineering and Technology,School of Electrical and Electronic Engineering, and State Key Laboratory ofMaterials Processing, and Die & Mould Technology, College of Materials Scienceand Engineering, Huazhong University of Science and Technology, Wuhan, Hubei,China 430074. E-mail: kjiang@hust.edu.cn; klwang@hust.edu.cn

†Electronic Supplementary Information (ESI) available: See DOI: 10.1039/x0xx00000x

† These authors contributed equally to this work

linked conducting-network for the polymer backbone, but also enable a robust structure to realize stable cycling performances.

In this paper, a polyimide-MWCNTs composite (PNP@CNTs) was prepared via a facile dehydration condensation reaction with the addition of MWCNTs, and investigated as a novel Na-storage anode in aqueous electrolyte for the first time. The as prepared PNP@CNTs demonstrated a high reversible capacity of 149 mAh g^{-1} at a quite low potential of - 0.65 V (vs SCE) with flat dicharge plateaus, superior rate capability at 20 C (1 C=100 mA g-1) and excellent cycling stability over 500 cycles, possibly serving as a low cost and cycling-stable organic anode for aqueous Na-ion batteries.

2. Experimental

2.1 Materials preparation

PNP@CNTs was synthesized by a facile dehydration condensation reaction as follows: A mixture of 2 mmol NTCDA (Aladdin, 99%) and 2 mmol PDA reacted under reflux in the solvent of 20 ml N-methyl-2-pyrrolidone (NMP) under inert atmosphere for 6 hours, cooled to room temperature. Then, 0.05 g MWCNTs were added into the above mixture and ultrasonic at 50 °C for 2 h. The product was filtrated, washed with deionized water and NMP for several times, dried under vacuum at 120 °C for 12 hours, then heated in nitrogen atmosphere for 6 hours at 300°C. The PNP polymer was synthesized in the same way as above without the addition of MWCNTs.

$Na_{0.44}MnO_2$ was prepared according to the method previously reported.[9] A typical experimental procedure was to dissolve 0.53 g Na_2CO_3, 4.9 g $Mn(Ac)_2$ and 1.05 g citric acid in distilled water and stir to obtain a clear and viscous gel. The resultant gel was dried at 120 °C for 12 h, heat-treated at 350°C for 4 h and 850 °C for 6 h in air to obtain the final product.

2.2 Structural Characterization

The morphology of the obtained samples were characterized using field-emission scanning electron microscopy (Zeiss SIGMA FESEM). Fourier transformed infrared (FTIR) spectra were recorded on a Bruker VERTEX 70 FTIR spectrometer with KBr pellets. Thermogravimetry analysis (TGA) were characterized on STA 449 F5-Jupiter from room temperature to 800 °C in N_2 with the heating rate of 10 °C min^{-1} . The specific surface area were determined by Brunauer–Emmett–Teller (BET) nitrogen adsorption–desorption measurement on TriStar II 3020.

For IR characterizations, the electrode samples at different charge and discharge states taken out from the disassembled cells were firstly rinsed with deionized water for several times and dried at 80 °C in vacuum for 60 min.

For ICP analysis of Na content, the dried electrode samples were burnt in a tubular furnace at 600 °C for 10 h. The as-obtained sodium oxide residue was then dissolved in HNO_3 for the atomic emission analysis using IRIS Intrepid Ⅲ XSP spectrometer.

2.3 Electrochemical Measurements

Electrochemical performances of PNP and PNP@CNTs electrodes were carried out using three-electrode cells. The working electrodes were made by pressing thin film (containing 60% active material, 30% conductive carbon and 10% polytetrafluroethylene binder) onto a Ti mesh. The counter electrode was a large piece of activated carbon and the reference electrode was saturated calomel electrode (0.24 v *vs* SHE). The electrolyte was a 1 M Na_2SO_4 solution (pH = 7) purged with Ar for several hours. The full aqueous cell was assembled in an argon-filled glove box (water/oxygen content lower than 1 ppm) with 2032 type coin cells, using $Na_{0.44}MnO_2$ as the cathode, PNP@CNTs as the anode (the mass ratio of cathode and anode is 2.5: 1), 1 M Na_2SO_4 solution (pH = 7) as the electrolyte. The galvanostatic charging-discharging experiments were conducted by a Land battery testing system(Wuhan Kingnuo Electronic Co., China) at various rates (1C = 100 mA g^{-1}) in the voltage range -1.0-0 V at room temperature. Cyclic voltammetry (CV) was carried out on a CHI 600e electrochemical workstation (Chen Hua Instruments Co).

3. Results and Discussion

The PNP polymer was synthesized via a facile dehydration condensation reaction as shown in Figure 1a**.** The as-prepared PNP is in the form of dark brown powder and almost insoluble in common organic or aqueous electrolytes.

The morphology of the as-prepared PNP and PNP@CNTs were further characterized by scanning electron microscopy (SEM). As shown in Figure 1, the PNP polymer appear as uneven agglomerates with large size of ~ 1 um (Figure 1b), while the PNP@CNTs composite emerges as well-defined particles of 100 nm particles cross-linked with CNTs (Figure 1c). It is well- established that the highly conductive MWCNTs network can provide abundant electrochemically active areas for Na^+ insertion/extraction reactions. The chemical structure of PNP was confirmed by FT-IR spectrometry. The FT-IR spectrum in Figure 1d reflects all the characteristic absorptions of a typical naphthalene-derived polyimide: such as the stretching vibration of the C–N (1344 cm^{-1}) and naphthalene ring

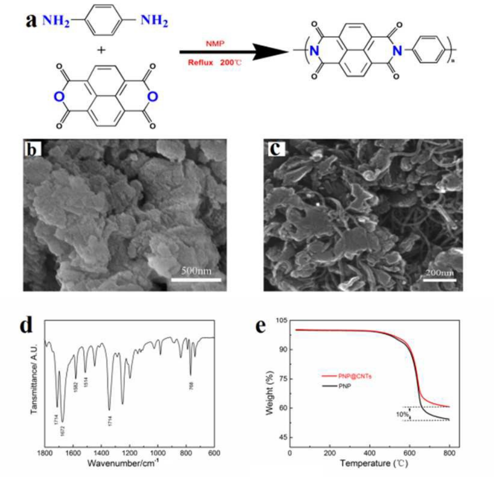

Fig. 1. (a) Synthetic route of the PNP polymer; (b) SEM imagine of the bare PNP, (c) PNP@CNTs composite; (d) FTIR spectrum of the PNP; (b) Thermogravimetric (TG) curves of PNP and PNP@CNTs in N_2 with heating rate of 10 °C min^{-1}.

(1582 cm $^{-1}$). The bands at 1714 cm $^{-1}$, 1672 cm $^{-1}$ and 768 cm $^{-1}$ are assigned to asymmetric and symmetric stretching vibrations of the C=O bond.

The characteristic stretching modes of the benzene ring (PDA) can be detected at 1514 cm $^{-1}$. The Brunauer-Emmett-Teller (BET) measurement suggests a mesoporous structure of the PNP particles, as evidenced by the nitrogen adsorption/desorption isotherms of IV type (Figure S1). Based on the BET analysis, the specific surface areas of the bulk PNP and PNP@CNTs were measured to be 8.7546, 24.8775 m ^{2} g $^{-1}$, respectively. Figure 1e presents the thermogravimetry analyses (TGA) curves of PNP and PNP@CNTs, the carbon contents in the PNP@CNTs is calculated to be ~10%.

The electrochemical reactivity of the PNP@CNTs was investigated by cyclic voltammetry (CV) at a scan rate of 2 mV s $^{-1}$. As shown in Figure 2b, the main CV features of the PNP@CNTs polymer appear as two pairs of well-defined redox peaks located at -0.78/-0.6 V and -0.58/-0.4 V (vs SCE), resembling very much the CV patterns of polyimide electrodes in organic electrolytes,[18] implying a reversible two-electron enolization reaction of the carbonyl group in the polyimide structure (Figure 2a). In addition, the two pairs of redox peaks appeared quite equally in the peak area, keeping almost unchanged during the subsequent cycles, suggesting excellent electrochemical reversibility and cycling stability. Noteworthy, in the first anodic scan, there is only one broad peak occurring at -0.78 V which can be attributed to an initial activation process of the polymer chains. As the activity of the polymer is associated with the polymer skeleton and the surface structure of the polymer particles, the as-prepared inert chains can be activated during the first few charge-discharge cycles.

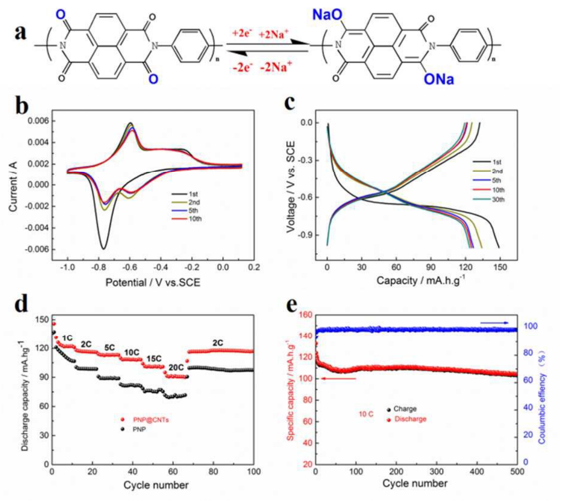

Fig. 2. (a) The reaction mechanism of the PNP@CNTs composite; (b) CV curves of PNP@CNTs measured at a scan rate of 2mv s $^{-1}$; (c) the charge-discharge profiles in the first 30 cycles at a current density of 1 C (100 mA g $^{-1}$); (d) reversible capacities at various current densities from 1 C to 20 C; (e) long-term cycling performances at a constant current density of 10 C. All the cells were cycled in the potential range from -1.0 and 0 V (vs SCE).

The electrochemical performance of the PNP@CNTs was further evaluated by galvanostatic charge-discharge cycling in 1 M Na_2SO_4 solution (PH=7) using three-electrode cells. Figure 2c shows the typical discharge-charge profiles of the PNP@CNTs electrode at the current density of 1 C (100 mA g $^{-1}$). In accordance with its CV features, the charge/discharge files of the polymer electrode shows planar voltage plateau at quite a low potential of - 0.65 V (vs SCE).

The charge and discharge capacities of PNP@CNTs in the first cycle are 149 and 132.3 mAh g $^{-1}$, corresponding to an initial columbic efficiency of 88.8% which is much higher than other aqueous organic anode reported previously.[19, 27] The coulombic efficiency rapidly rose up to ~100% in the subsequent cycles and the reversible capacity of the PNP@CNTs anode decreases slowly in the first 5 cycles and remains stable at ~125 mAh g $^{-1}$. The capacity decrease in the first few cycles can be ascribed to the slight solubility of the reduction products of the oligomers in aqueous electrolytes. It is worth noted that the high initial coulombic efficiency, low redox potential and high reversible capacity of the PNP@CNTs guarantee the feasibility of its practical application as aqueous Na-storage anode.

In addition to the dramatically high capacity, the PNP@CNTs electrode also exhibits superior high rate capability and long cycling stability. Figure 2d compares the rate capability of the PNP and PNP@CNTs electrodes. The PNP@CNTs electrode delivers a reversible capacity of 132, 120, 115, 110, 102 mAh g $^{-1}$ at different current densities of 1, 2, 5, 10, 15 C (1 C= 100 mA g $^{-1}$), respectively. Even at a very high current density of 20 C, a capacity of ~92 mA h g $^{-1}$ is still delivered, corresponding to 70% of the capacity obtained at 1 C. In contrast, the PNP electrode shows much poor rate performances and the reversible capacity is rapidly declined to less than 70 mA h g $^{-1}$ when the current density increases to 20 C (50% of that obtained at 1 C), indicating a significant enhancement in rate capability of the PNP after hybridized with MWCNTs. The excellent rate capability of the PNP@CNTs can be attributed to the unique structure of the highly conjugated polymer skeleton interconnected with conductive CNTs network, which can not only facilitate the Na $^+$ diffusion with a low ion-transport resistance restrictions, but also ensure an efficient and continuous path for electron transport. The long-term cycling performances of the PNP@CNTs was further

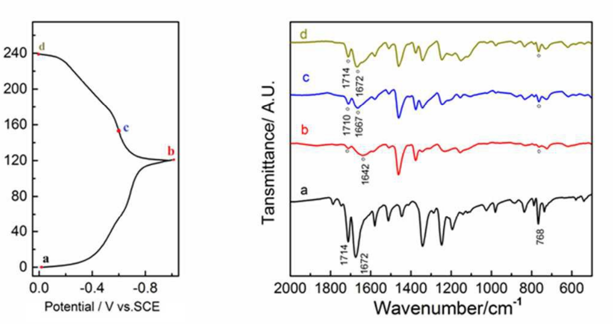

Fig. 3. FT-IR spectra of the PNP@CNTs electrode (right) recorded at different potentials as indicated in the charge and discharge curve (left): (a) as-prepared PNP@CNTs electrode; (b) discharge to -1 V; (c) Charge to -0.6 V and (d) Charge to 0 V (vs SCE).

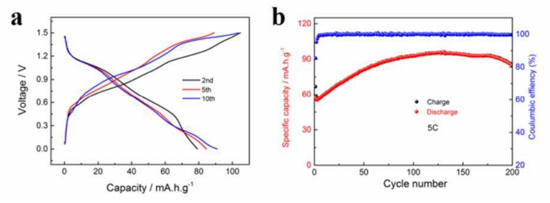

Fig. 4. Electrochemical performances of the PNP@CNTs/NMO full cell: (a) the charge-discharge profiles in first ten cycles at a current density of 1 C; (b) long-term cycling stability at a constant current of 5 C (1 C=100 mA g^{-1}).

evaluated at a high current density of 10 C. As shown in Figure 2e, the reversible capacity of the PNP@CNTs anode decreases slowly during the first 10 cycles and then remains stable over the subsequent 500 cycles. In addition, the coulombic efficiency stabilized to > 99 % after a few cycles, indicating a stable electrochemical reversibility. The outstanding cyclability of the PNP@CNTs electrode should be benefited from the robust structure of the PNP@CNTs electrode originated from the large π-conjugated polymer backbone and high mechanical strength of the carbon additives (CNTs).

In order to further confirm the carbonyl enolization reaction mechanism described above, ex-situ FT-IR analysis was carried out to characterize the changes in the bonding states of the PNP backbones at different depths of charge and discharge. As shown in Figure 3, the pristine electrode presents a typical adsorption pattern of the as-prepared PNP. When first discharged to -1.0 V, the bands at 1714 (C=O), 1672(C=O) cm^{-1} were almost indiscernible, while the peaks at 1642 cm^{-1} appeared, reflecting a total conformational change of the carbonyl groups to the enol structure. When charged to -0.6 V, the band of the C=O bond reemerged but shifted to 1710 and 1667 cm^{-1}, suggesting a partial oxidation of the enol structure to the C=O structure. At the fully charged state of 0 V, all the bands recovered to the original positions, implying a high reversibility of the enolization reaction of the carbonyl groups in the PNP structure. Furthermore, the quantitative ICP characterization of the PNP@CNTs electrode confirmed the enolazation reaction of 2 Na storage reaction mechanism in the polymer anode.

To evaluate the practical feasibility of the polymer as an anode for aqueous Na-ion batteries, an aqueous Na-ion full cell was fabricated using $Na_{0.44}MnO_2$ (NMO) as the cathode and PNP@CNTs as the anode. NMO was synthesized by solid-state reaction as described in the experiment section. The NMO cathode demonstrates a reversible capacity of ~40 mAh g^{-1} at average potential of ~ 0.25 V (vs SCE) (see Supporting Information Figure S3). Figure 4 demonstrates the charge/discharge profiles of the coin type PNP@CNTs/NMO battery. This aqueous Na-ion full battery shows a discharge voltage of 0.8 V and delivers a reversible capacity of 92 mAh g^{-1} in terms of anode capacity. This cell can be well cycled at a high rate of 5 C (1 C = 100 mA g^{-1}) over 200 cycles, delivering the energy density of 25 Wh Kg^{-1}, suggesting a possible application of the PNP@CNTs composite as an organic anode for practical aqueous Na-ion full battery applications. Particularly, the coulombic efficiency of the full cell increase rapidly closed to 100% in the first 5 cycles, implying a very high electric energy conversion efficiency which is of great concern for the practical electric storage applications.

4. Conclusions

In summary, we prepared a PNP@CNTs composite facilely by polycondensation method with the addition of MWCNTs, and investigated it as Na-storage anode in aqueous electrolyte for the first time. Based on the robust structure and high conductivity of the PNP@CNTs electrode, this composite electrode exhibits a remarkable electrochemical performance with a high reversible capacity of 149 mAh g^{-1} at quite a low potential of -0.65 V (vs SCE), outstanding rate capability and excellent long-term cycling stability. Particularly, the environmental friendliness, low cost and simple synthesis of the organic compound enables it as promising Na storage anode for aqueous Na-ion batteries for widespread electrical energy storage applications.

Acknowledgment

This work was supported by the Natural Science Foundation of China (Grant 21503084), 973 Program (2015CB258400) and the National Thousand Talents Program of China.

Notes and references

1. B. Dunn, H. Kamath, J. M. Tarason, *Science* 2011, **334**, 928-935.
2. Z. Yang, J. Zhang, M. C. Kintner-Meyer, X. Lu, D. Choi, J. P. Lemmon, J. Liu, *Chem. Rev.* 2011, **111**, 3577–3613.
3. H. Pan, Y. –S. Hu, L. Chen, *Energy Environ. Sci.* 2013, **6**, 2338-2360.
4. N. Yabuuchi, K. Kubota, M. Dahbi, S. Komaba, *Chem. Rev.* 2014, **114**, 11636-11682.
5. H. Kim, J. Hong, K. Park, S. W. Kim, K. Kang, *Chem. Rev.* 2014, **114**, 11788-11827.
6. D. J. Kim, R. Ponraj , A. G. Kannan , H.-W. Lee , R. Fathi , R. Ruffo , C. M. Mari , D. K. Kim , *J. Power Sources* 2013 , **244** , 758-763.
7. W. Choi, D. Harada, K. Oyaizu, H. Nishide, *J. Am. Chem. Soc.* 2011, **133**, 19839–19843.
8. S. Komaba, A. Ogata, T. Tsuchikawa. *Electrochem. Commun.* 2008, **10**, 1435−1437.
9. J. Whitacre, A. Tevar, S. Sharma. *Electrochem. Commun.* 2010, **12,** 463−466.
10. X. Wu. Y. Luo, M. Sun, J. Qian, Y. Cao, X. Ai, H. Yang, *Nano Energ.* 2015, **13**, 117-123.
11. X. Wu, M. Sun, Y. Shen, J. Qian, Y. Cao, X. Ai and H. Yang, *ChemSusChem*, 2014, **7**, 407-411.
12. X. Wu, Y. Cao, X. Ai, J. Qian and H. Yang, *Electrochem. Commun.* 2013, **31**, 145-148.
13. S. Park, I. Gocheva, S. Okada*,* J. Yamaki, *J. Electrochem. Soc.* 2011, **158***,* A1067−A1070.
14. W. Wu, A. Mohamed, J. F. Whitacre, *J. Electrochem. Soc.* 2013, **160,** A497−A504.
15. Z. Li, D. Young, K. Xiang*, et al, Adv. Energy Mater.* 2013, **3***,* 290−294.

16. K. Koshika, N. Sano, K. Oyaizu*, Chem.Commun.* 2009, **7***,* 836–838.
17. D. Kim , Y. Jung , K. Bharathi , S. Je , D. Kim , A. Coskun , J. Choi, *Adv. Energ. Mater.* 2014, **4***,* 1400133.
18. Z. Song, H. Zhan, Y. Zhou, *Angew. Chem. Int. Ed.* 2010**, 49***,* 8444–8448.
19. H. Qin , Z. P. Song , H. Zhan , Y. H. Zhou , *J. Power Sources* 2014 , **249** ,367-372.
20. M. Zhou, W. Li, T. T. Gu, K. L. Wang, S. J. Cheng, K. Jiang, *Chem. Commun.* 2015, **51**, 14354-14357.
21. L. Chen, W. Y. Li, Y. G. Wang, C. X. Wang, Y. Y. Yao, *RSC Advances* 2014, **4,** 25369-25373.
22. Z. P. Song, H. Zhan, Y. H. Zhou, Chem. Commun. 2009, 448-450.
23. W. Deng, X. Liang, X. Wu, J. Qian, Y. Cao, H. Yang, Sci. Rep. 2013, 3, 2671.
24. F. Xu, J. Xia, W. Shi, *Electrochem. Commun.* 2015, *60*, 117-120.
25. H. Banda, D. Damien, K. Nagarajan, M. Hariharanb, M. Shaijumon, *J. Mater. Chem. A*, 2015, **3**, 10453-10458.
26. H. Wang, S. Yuan, D. Ma, X. Huang, F. Meng, X. Zhang, *Adv. Energ. Mater.* 2014, **4**, 1-7.
27. W. Deng, Y. Shen, J. Qian, H. Yang, *Chem. Commun.* 2015, **51**, 5097-5099

GRAPHICAL ABSTRACT

AUTHOR NAMES: Tiantian Gu [†], Min Zhou[†], Mengyun Liu, Kangli Wang*, Shijie Cheng, Kai Jiang*

TITLE : A Polyimide-MWCNTs composite as high performance anode for aqueous Na-ion batteries.

Benefiting from its highly conjugated structure and robust conducting network, the PNP@CNTs electrode demonstrates a high reversible capacity of 149 mAh g^{-1} at quite a low potential of -0.65 V (vs SCE), superior rate capability and long-term cycling stability over 500 cycles, possibly serving as a low cost and high performance Na host anode for aqueous Na-ion batteries.

GRAPHICAL ABSTRACT FIGURE